Arts Syndrome Is Caused by Loss-of-Function Mutations in *PRPS1*

Arjan P. M. de Brouwer, Kelly L. Williams, John A. Duley, André B. P. van Kuilenburg, Sander B. Nabuurs, Michael Egmont-Petersen, Dorien Lugtenberg, Lida Zoetekouw, Martijn J. G. Banning, Melissa Roeffen, Ben C. J. Hamel, Linda Weaving, Robert A. Ouvrier, Jennifer A. Donald, Ron A. Wevers, John Christodoulou, and Hans van Bokhoven

Arts syndrome is an X-linked disorder characterized by mental retardation, early-onset hypotonia, ataxia, delayed motor development, hearing impairment, and optic atrophy. Linkage analysis in a Dutch family and an Australian family suggested that the candidate gene maps to Xq22.1-q24. Oligonucleotide microarray expression profiling of fibroblasts from two probands of the Dutch family revealed reduced expression levels of the phosphoribosyl pyrophosphate synthetase 1 gene (*PRPS1*). Subsequent sequencing of *PRPS1* led to the identification of two different missense mutations, c.455T→C (p.L152P) in the Dutch family and c.398A→C (p.Q133P) in the Australian family. Both mutations result in a loss of phosphoribosyl pyrophosphate synthetase 1 activity, as was shown *in silico* by molecular modeling and was shown in vitro by phosphoribosyl pyrophosphate synthetase activity assays in erythrocytes and fibroblasts from patients. This is in contrast to the gain-of-function mutations in *PRPS1* that were identified previously in PRPS-related gout. The loss-of-function mutations of *PRPS1* likely result in impaired purine biosynthesis, which is supported by the undetectable hypoxanthine in urine and the reduced uric acid levels in serum from patients. To replenish low levels of purines, treatment with *S*-adenosylmethionine theoretically could have therapeutic efficacy, and a clinical trial involving the two affected Australian brothers is currently underway.

Phosphoribosyl pyrophosphate synthetase 1 (PRS-I) is a member of a family of phosphoribosyl pyrophosphate (PRPP) synthetases that catalyze the synthesis of PRPP from ATP and ribose-5-phosphate.[1] PRPP is essential for de novo purine and pyrimidine synthesis. In men, there are three genes for the PRPP synthetase family—*PRPS1* (MIM 31185), *PRPS2* (MIM 311860), and *PRPS1L1*—all of which encode nearly (>90%) identical proteins. *PRPS1* and *PRPS2* have multiple exons and map to the long and short arms of the X chromosome, respectively. *PRPS1L1* is an intronless gene located on chromosome 7 that appears to have arisen through retrotransposition of a spliced *PRPS1* or *PRPS2* transcript. The expression of *PRPS1L1* is limited to testis,[2] whereas *PRPS1* and *PRPS2* are expressed in all tissues.[3]

Previously described missense mutations in *PRPS1* cause PRPP synthetase superactivity, which results in PRPS-related gout (MIM 311850).[1] In addition, overexpression of *PRPS1* causes the same syndrome, although the underlying mechanism remains elusive.[4] PRPS-related gout is characterized by purine nucleotide and uric acid overproduction,[5–7] gout,[6,8] and sometimes neurological problems, most notably mental retardation, hypotonia, and sensorineural deafness.[8–11] PRPS-related gout is 1 of the 14 different known disorders caused by inborn errors of purine and pyrimidine metabolism.[12] The accumulation of purines to toxic levels can result in a variety of clinical symptoms, such as renal stones, gouty arthritis, developmental delay, hypotonia, and immunodeficiency. Susceptibility to infections and developmental delay are also seen in disorders of pyrimidine metabolism, such as orotic aciduria (MIM 258900) and pyrimidine nucleotide depletion.[12,13]

Arts syndrome (MIM 301835) is defined by mental retardation, early-onset hypotonia, ataxia, delayed motor development, hearing impairment, and optic atrophy.[14] Susceptibility to infections, especially of the upper respiratory tract, can result in an early death. Interestingly, Arts syndrome shows characteristics in common with purine-overproduction disorders, such as mental retardation, delayed motor development, ataxia, sensorineural impairment, and recurrent infections, symptoms that occur in patients with hypoxanthine guanine phosphoribosyltransferase (HPRT1) deficiency (MIM 300322), purine nucleoside phosphorylase (PNP) deficiency (MIM 164050), and PRPP synthetase superactivity.[12] However, Arts syndrome lacks evidence of purine overproduction, since patients do not develop renal stones or gout (authors' unpublished observations).

Here, we report that Arts syndrome is caused by missense mutations in *PRPS1*. In contrast to PRPS-related

From the Departments of Human Genetics (A.P.M.d.B.; M.E.-P.; D.L.; M.J.G.B.; M.R.; B.C.J.H.; H.v.B.) and Neurology (R.A.W.), Radboud University Nijmegen Medical Centre, and Centre for Molecular and Biomolecular Informatics, Radboud University Nijmegen (S.B.N.), Nijmegen, The Netherlands; Department of Biological Sciences, Macquarie University (K.L.W.; J.A.D.), Western Sydney Genetics Program (L.W.; J.C.) and TY Nelson Department of Neurology and Neurosurgery (R.A.O.), Children's Hospital at Westmead, and Discipline of Paediatrics and Child Health, University of Sydney (R.A.O.; J.C.), Syndey; School of Pharmacy, University of Queensland (J.A.D.), and Department of Pathology, Mater Hospital (J.A.D.), Brisbane, Australia; and Emma Children's Hospital and Department of Clinical Chemistry, Academic Medical Center, University of Amsterdam, Amsterdam (A.B.P.v.K.; L.Z.)

Received May 17, 2007; accepted for publication June 4, 2007; electronically published August 3, 2007.

Address for correspondence and reprints: Dr. Arjan P. M. de Brouwer, Department of Human Genetics, Radboud University Nijmegen Medical Centre, P.O. Box 9101, 6500 HB Nijmegen, The Netherlands. E-mail: A.debrouwer@antrg.umcn.nl

Am. J. Hum. Genet. 2007;81:507–518. 0002-9297/2007/8103-0008$15.00
DOI: 10.1086/520706

gout, the missense mutations in Arts syndrome cause a loss of function, which was validated *in silico* by molecular modeling; in vitro by PRPP synthetase activity assays in erythrocytes, Epstein-Barr virus–transformed lymphoblastoid cell lines (EBV-LCLs), and skin fibroblasts from patients and carrier females; and in vivo by analysis of metabolites in urine and plasma from patients and carrier females. These results emphasize the importance of the tight regulation of PRPP synthetase activity and that increased or reduced activity can give rise to clinically distinct human disorders.

Material and Methods

Genetic Mapping of Australian Family F

DNA from family F was extracted from peripheral whole blood by the salting-out method as described by Miller et al.[15] Preliminary X-chromosome mapping in family F was performed using the ABI Prism set version 2, panel 28 (X chromosome), obtained from Applied Biosystems. This set comprised primers for 18 fluorescently labeled microsatellite markers dispersed at intervals of ~10 cM over the entire X chromosome. Markers for the fine mapping of the candidate regions were spaced at 0.4–5 cM. The forward primers for these microsatellites were fluorescently labeled with Fam, Hex, or Ned. PCR conditions were optimized for individual primers and are available on request.[16] PCRs were performed in a 9600 thermocycler (Applied Biosystems). The programs used were 95°C for 12 min for one cycle, followed by 35 cycles of melting at 94°C for 15 s, annealing at the optimal temperature for 15 s, and then extension at 72°C for 30 s. A final extension was performed at 72°C for 4 min. PCR products were run on an ABI 377 sequencer (Applied Biosystems). Exclusion mapping was used to identify candidate regions on the X chromosome under the following assumptions: alleles not shared between the two affected brothers were excluded, alleles shared between the affected brothers and their unaffected maternal uncle were excluded, and alleles inherited from the maternal grandfather were excluded.

Cell Culturing

Skin fibroblast cell lines were cultured in Dulbecco's modified Eagle's medium (DMEM [Gibco]) supplemented with 20% (v/v) fetal calf serum (Sigma), 1% 10-U/μl penicillin with 10-μg/μl streptomycin (Gibco), 1% GlutaMAX (Gibco), and 1 mM sodium pyruvate (Gibco). Cells were harvested at 80%–90% confluence for both RNA isolation and PRPP synthetase activity analysis by washing once with PBS buffer (8 mM Na_2HPO_4, 2 mM KH_2PO_4, 137 mM NaCl, and 2.7 mM KCl [pH 7.2]), followed by treatment with 0.25% trypsin (Sigma) in PBS. Cells were centrifuged at 200 *g* for 5 min at room temperature, were washed with PBS, and were pelleted by centrifugation at 200 *g* for 5 min at room temperature. This last step was repeated for PRPP synthetase activity analysis. Pellets for both RNA isolation and enzyme activity analysis were immediately snap frozen in liquid nitrogen.

Human B-lymphocytes were immortalized by transformation with Epstein-Barr virus in accordance with established procedures.[17] EBV-LCLs from patients and controls were grown to a density of 0.7 million cells per ml RPMI 1640 medium (Gibco) containing 10% (v/v) fetal calf serum (Sigma), 1% 10-U/μl penicillin and 10-μg/μl streptomycin (Gibco), and 1% GlutaMAX (Gibco). A total of 25 million cells were harvested by centrifugation at 200 *g* for 5 min at room temperature, were washed with PBS, and were pelleted by centrifugation at 200 *g* for 5 min at room temperature. The pellets for enzyme activity analysis were immediately snap frozen in liquid nitrogen.

RNA Isolation

Total RNA was isolated using the RNeasy Mini Kit (Qiagen) in accordance with the manufacturer's protocol. To remove residual traces of genomic DNA, the RNA was treated with DNase I (Invitrogen) while bound to the RNeasy column. The integrity of the RNA was assessed on an agarose gel, and the concentration and purity were determined by optical densitometry. Poly-A^+ RNA was isolated using the Oligotex Direct mRNA Kit (Qiagen) in accordance with the manufacturer's protocol.

Expression Profiling

Total RNA from eight healthy control males and females was divided into two reference pools consisting of four different samples. These served as references to establish differential gene expression in fibroblast cell lines of the two affected members of family N032. GeneChip expression analysis using the GeneChip Human Genome U133 Plus 2.0 Array was performed in accordance with the manufacturer's protocol (Affymetrix) by use of total RNA and the one-cycle target-labeling assay. Data from both affected family members were averaged and were compared with the combined reference data by use of Genespring (Agilent Technologies). Probe sets that had a signal value <100 were regarded as "not expressed." In addition, probe sets with probes in intronic sequences that were not supported by human mRNAs from GenBank or by spliced ESTs were not considered. If a probe set was reduced in expression, the probes in that particular set were checked for redundancy and were discarded if more than half the probes in the set could bind to more than one transcript. When multiple probe sets were present for one transcript, at least two had to be reduced in expression.

First-Strand Synthesis for Quantitative PCR (qPCR)

The poly-A^+ RNA equivalent of 5 μg of total RNA was transcribed into cDNA as follows. Poly-A^+ RNA (0.2 μg total RNA/μl), 0.05 U/μl $pd(N)_6$ (Amersham Biosciences), and 1 mM deoxyribonucleotide triphosphate (dNTP) (Invitrogen) were incubated for 5 min at 65°C. The mixture was then cooled on ice for 1 min. First-strand buffer (Invitrogen), 10 mM dithiothreitol, and 0.5 U/μl RNA Guard (Amersham Biosciences) were added. One-tenth of the reaction mixture served as the minus–reverse transcriptase control. M-MLV reverse transcriptase (Invitrogen) was added for a final concentration of 10 U/μl. This solution was, in subsequent steps, incubated at 25°C for 10 min, at 50°C for 50 min, and at 70°C for 15 min. cDNA was purified using QIAquick columns (Qiagen) in accordance with the manufacturer's protocol.

qPCR

qPCR was performed by SYBR Green–based quantification in accordance with the manufacturer's protocol (BioRad) by use of an iCycler (MyiQ single-color real-time detection System [BioRad]). Primers were developed using the Primer3 program.[18] In the case of *GUSB* (MIM 253220) and *CUL4B* (MIM 300304), the primers were designed on two separate exons. *GUSB* is stably expressed

in fibroblasts and thus is a good reference gene to use.[19] Since *PRPS1* and *PRPS2* are very similar, primers had to be designed that anneal to the 3′ UTR of these genes. Sequences of the qPCR primers are shown in table 1. PCR products were 80–120 bp in length. All primer pairs were validated in triplicate by use of serial cDNA dilutions that result in end concentrations equivalent to 800, 400, 200, 100, and 50 pg/μl of total RNA input into the first-strand synthesis. Primers that were 100% ± 5% efficient, which implies a doubling of PCR product in each cycle, were used to quantify mRNA levels. qPCR quantifications were performed with the equivalent of 400 pg/μl of total RNA input into the first-strand synthesis from two separate first-strand syntheses each in duplicate, and they included a water or minus–reverse transcriptase control. The quantification was repeated on separately grown cell lines, and the results were averaged. Experimental threshold cycles (Ct) values were within the range of cDNA dilutions used to validate the primers. The melting curves of all PCR products showed a single PCR product. All controls were negative. Differences in the expression of a gene of interest between two samples were calculated by the comparative Ct or $2^{\Delta\Delta Ct}$ method.[20,21]

Mutation Analysis

Primer sequences for amplification of all exons of *CUL4B* (GenBank accession number NM_003588.3) and *PRPS1* (GenBank accession number NM_002764.2) are shown in table 1. Of the last exon of *CUL4B* and *PRPS1,* 210 nt and 750 nt of the 3′ UTR were analyzed, respectively. PCR conditions are available on request. PCR products were sequenced using the ABI PRISM BigDye Terminator Cycle Sequencing version 2.0 Ready Reaction Kit and were analyzed using the ABI PRISM 3730 DNA analyzer (Applied Biosystems). In the case of *TRPC5* (GenBank accession number NM_012471.2; MIM 300334), the entire coding region of the candidate gene was amplified using the methods of Sossey-Alaoui et al.[22] Automated ABI 377 sequencing was performed using both forward and reverse primers from each PCR.

The segregation of the c.455T→C nucleotide change in *PRPS1* in family N032 and its presence in 169 healthy males and 70 healthy females were tested by amplification of exon 4 and subsequent digestion by *Bsm*FI in accordance with the manufacturer's protocols (Invitrogen). The segregation of nucleotide sub-

Table 1. Sequences of Primers Used for qPCR and Direct DNA Sequencing

Procedure and Gene or Exon	GenBank Accession Number	Primer Sequence (5′→3′)	
		Forward	Reverse
qPCR:			
PRPS1	NM_002764.2	gatctatttggcctctcaaa	cacacaggtacacacactttatt
PRPS2	NM_002765.3	ggacctgcatgcttctcag	atgttttcccgaatccactg
CUL4B	NM_003588.3	accaccgtctctagctttgc	tttgccaggtttcatctgtg
GUSB	NM_000181.1	agagtggtgctgaggattgg	ccctcatgctctagcgtgtc
Direct DNA sequencing:			
CUL4B exon 1.1	NM_003588.3	cactaccctgatgcaccacc	tgtatttaacaccttccggg
CUL4B exon 1.2	NM_003588.3	tcttttggctccaaccagg	ccaggtccaccttcaataag
CUL4B exon 2	NM_003588.3	attggctgggaaaccagag	cctgacctcgtgatctgctc
CUL4B exon 3.1	NM_003588.3	acgcacgcaggcatataaac	caaaccctacaaactccaggg
CUL4B exon 3.2	NM_003588.3	cttcaacctcgtccttctgc	gacccctcgagtgtcaaatc
CUL4B exon 4	NM_003588.3	ggtgagtcaaaatgacttaaacag	cccatggtttatgtgagaatacg
CUL4B exon 5	NM_003588.3	tgtcttaagtggatgaataaccc	gctgggttaaacagtgaggg
CUL4B exon 6	NM_003588.3	tatgctctctgtcacatggc	gaagcaatctccctattgctaag
CUL4B exon 7	NM_003588.3	tagatgtgtttatctgcatgtttg	caaaggaaagtctagaaccaaatg
CUL4B exon 8	NM_003588.3	aattagcatgggaacatgtgg	cattacctgtctgatgtgggg
CUL4B exon 9	NM_003588.3	acaaaaggatcctagcttgatg	gagaagagcatcacaatgttgg
CUL4B exon 10	NM_003588.3	ccacttccaggatcttttgg	tgctgcaagtgatttaacgac
CUL4B exon 11	NM_003588.3	cccctcaggagaggctttac	ttccctactagtttgccactacc
CUL4B exon 12	NM_003588.3	tacccagaaagatggttggg	tcaaacaagaaatgcttgcc
CUL4B exon 13	NM_003588.3	tggggattgttttcattgtag	cttgatataccagctaagcaacc
CUL4B exon 14	NM_003588.3	cccagtacctcgtgtattccc	tccctccagtttgaatatacttg
CUL4B exon 15	NM_003588.3	agacttcgaaatgtctggcac	gaggaaatcgattgaaaggg
CUL4B exon 16	NM_003588.3	tcgtgtttcccacttttaaacc	gccatgaattacaacaaacacg
CUL4B exon 17	NM_003588.3	tttaaggatggtcagtgtttgc	caatacagcgagaccctgg
CUL4B exon 18	NM_003588.3	tttgatttggtggttgggag	gcggtgagccaagatagc
CUL4B exon 19	NM_003588.3	taccacgtcaagtggctttg	caaaacagttctgaggcaagg
CUL4B exon 20	NM_003588.3	tggagtggaagctagattgagg	aatggtattggcagtattacagg
CUL4B exon 21	NM_003588.3	caatgtcatgtccctaaaatgc	tcatgacgctttatgtttgc
CUL4B exon 22	NM_003588.3	ggggtattaactaaatgggcttg	tgcaaagagttcaacaacattc
PRPS1 exon 1	NM_002764.2	tgagtctgtggccgacttc	cgaccccatccctcctatac
PRPS1 exon 2	NM_002764.2	tcaatccacacttggttgaatc	tccagaggagttggtgcttag
PRPS1 exon 3	NM_002764.2	atgaatttctgggtaccatagtg	cttctctgcagtcttcagcatc
PRPS1 exon 4	NM_002764.2	aatctaccacactgggcctg	ccatgtgctagctacttacatcc
PRPS1 exon 5	NM_002764.2	ccccggcctctttagtcc	tcagcaggctgaagacattc
PRPS1 exon 6	NM_002764.2	gttgtggaagcctaagcagg	cttcagaatccagagacctaattc
PRPS1 exon 7.1	NM_002764.2	tcatgacagggaaacagcac	gagcttccccagtcacagtc
PRPS1 exon 7.2	NM_002764.2	ttaactgctgggacctcctac	gaagcatgtttgctttccag

stitution c.398A→C in *PRPS1* in family F and its presence in 154 healthy females were tested by amplification of exon 3 and subsequent digestion with *Apo*I in accordance with the manufacturer's protocols (Invitrogen).

Molecular Modeling

The effect of the p.Q133P and p.L152P mutations on the structure of PRS-I was examined using the crystal structure of human PRPS1 from Li et al.[23] (RCSB Protein Data Bank entry 2H06). The altered amino acid side chains in the model were positioned using a backbone-dependent rotamer library as implemented in the Yet Another Scientific Artifical Reality Application (YASARA) program. The models were subsequently refined using the Yamber2 force field, which elsewhere was shown to increase model accuracy.[24] Coordinate files are available from the authors on request.

PRPP Synthetase Activity Analysis

PRPP synthetase activity in erythrocytes is based on high-performance liquid chromatography (HPLC) measurement of adenosine monophosphate (AMP), which is produced from the enzyme reaction in equimolar amounts with PRPP. The assay contains diadenosine pentaphosphate (A2P5), which inhibits dephosphorylation of ATP and adenosine diphosphate (ADP) by nonspecific phosphatases. In brief, erythrocytes were washed in saline and were stored frozen until required. For the assay, 100 μl of packed erythrocytes were lysed by freeze thawing in 500 μl buffer comprising 10 mM Tris-HCl (pH 7.5), 1 mM dithiothreitol, and 1 mM EDTA. Centrifuged lysate was dialyzed to remove erythrocyte nucleotides, by passing through a Sephadex G-25 column equilibrated with the lysis buffer mentioned above containing 0.9% (w/v) NaCl. The 150-μl assay mixture contained 50 mM Tris-HCl, 0.5 mM ATP, 0.25 mM ribose-5-phosphate, 0.25 mM A2P5, 1 mM dithiothreitol, 5 mM $MgCl_2$, and inorganic phosphate that varied in concentration from 0 to 32 mM. Each assay was commenced by the addition of 50 μl of dialyzed hemolysate and was incubated for 20 min at 37°C. The reaction was terminated by the addition of trichloroacetic acid, and the supernatant was subjected to ion-pair HPLC to separate the AMP.[25]

Frozen EBV-LCL and fibroblast pellets were suspended in 300 μl 0.9% (w/v) NaCl and were sonicated three times at 4 W for 10 s, with intervals of 30 s under constant cooling in ice water. After centrifugation (11,000 *g* at 4°C for 20 min), 250 μl of the supernatant was diluted with 250 μl 0.9% (w/v) NaCl and was concentrated on a Microcon YM-10 filter (Millipore) by centrifugation (14,000 *g* at 4°C for 60 min). The protein fraction was diluted to a final volume of 500 μl, with 0.9% (w/v) NaCl, and was concentrated again by centrifugation. The final concentrated protein fraction was saved, and the protein concentration was determined with a copper-reduction method using bicinchonic acid, essentially as described by Smith et al.[26] The activity of PRPP synthetases in EBV-LCLs was determined in a reaction mixture containing an aliquot of cell sample (0.05–0.65 mg), 40 mM sodium phosphate, 1 mM dithiothreitol, 6 mM $MgCl_2$, 1.54 mM ATP, 100 μM ribose-5-phosphate, 50 μM P^1,P^5-di(adenosine-5′)pentaphosphate (Ap5A), and 50 mM Tris/MOPS (pH 7.4). The activity of PRPP synthetases in fibroblasts was determined in a reaction mixture containing an aliquot of cell sample (0.02–0.032 mg), 32 mM sodium phosphate, 1 mM dithiothreitol, 5 mM $MgCl_2$, 0.5 mM ATP, 150 μM ribose-5-phosphate, 250 μM Ap5A, and 50 mM Tris/HCL (pH 7.4).[27] Separation of AMP, ADP, and ATP was performed isocratically (30% 0.0075-mM sodium phosphate to 70% 0.75-mM sodium phosphate [pH 4.55]) at a flow rate of 0.8 ml/min by HPLC on an ion-exchange column (Whatman Partisphere SAX 125 × 4.6 mm; 5 μm particle size [VWR International]) and a guard column (Whatman Partisphere AX 10 × 2.5 mm; 5 μm particle size [VWR International]) with online UV detection at 254 nm.

Metabolite Analysis in Urine

Urine and plasma purines and pyrimidines were determined using reversed-phase HPLC analysis as described elsewhere,[28] with the modification that a 250 × 3.1 mm (3μ) Synergi RP80A C18 column (Phenomenex) was used. Purine and pyrimidine metabolites were identified by their retention times and spectra (230–330 nm) by photodiode array detection.

Results

Clinical Description

In this article, two families with Arts syndrome were investigated. Family N032 is the original Dutch family described extensively by Arts et al.[14] In short, the syndrome is defined by mental retardation, early-onset hypotonia, ataxia, delayed motor development, hearing impairment, and optic atrophy (table 2). Susceptibility to infections, in particular of the upper respiratory tract, resulted in an early death, before age 5 years, for 9 of the 10 affected males in this family. Only one patient lived beyond age 5 years, reaching age 18 years. The CNS of one patient was examined at autopsy. In the posterior columns of the spinal cord, an almost complete absence of myelin was found. Carrier females from family N032 show isolated and milder manifestations of symptoms of Arts syndrome, such as perceptive hearing impairment, ataxia, hypotonia, and hyperreflexia.

The Australian family (family F) was ascertained independently (for pedigree, see fig. 1*A*). The two affected boys, III-2 and III-3, have mental retardation, hypotonia, ataxia, profound congenital sensorineural deafness, progressive peripheral neuropathy, and optic atrophy. They

Table 2. General Clinical Description of the Two Families with Arts Syndrome

Clinical Symptom	Family N032	Family F	PRPS1-Related Gout
Mental retardation	+	+	+
Ataxia	+	+	+
Hypotonia	+	+	+
Delayed motor development	+	+	+
Recurrent infections	+	+	−
Hearing impairment	+	+	+
Optic atrophy	+	+	−
Areflexia	+	+	+
Loss of deep tendon reflexes	+	+	−
Gout	−	−	+
Kidney stones	−	−	+
Early death	+	+	−

NOTE.—A positive sign (+) indicates the presence of the symptom; a negative sign (−) indicates the absence of the symptom.

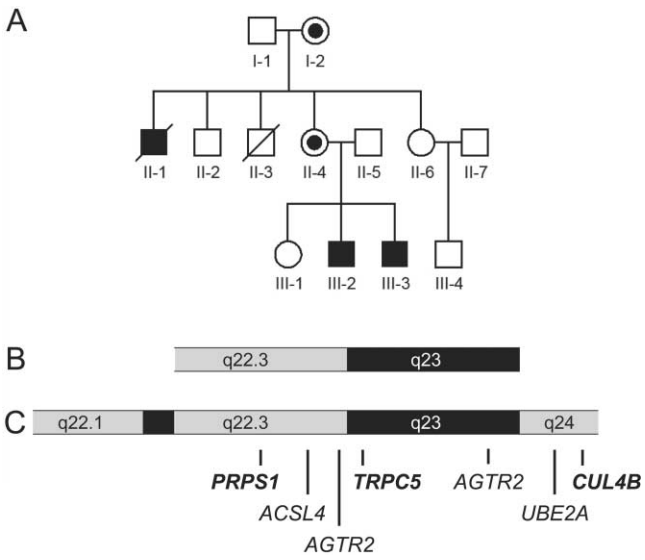

Figure 1. Pedigree of family F (*A*) and the overlapping linkage intervals between family F (*B*) and family N032 (*C*). Indicated are the positions of the genes analyzed in patients as described in this article (*bold font*) and as previously described by de Brouwer et al.[29]

also displayed slowly progressive muscle weakness associated with intermittent acute deterioration in muscle strength during intercurrent illnesses. The acute episodes of muscle weakness resulted in respiratory failure, requiring mechanical ventilation for a period of time. Both boys had delayed motor-nerve conduction velocities and an electromyogram suggestive of denervation, which is consistent with the clinical findings that suggested peripheral neuropathy. In addition, the younger boy had a fibrosing pancreatitis, the cause of which was never established. A sural nerve biopsy in the older boy revealed mild paranodal demyelination. Other investigations with normal findings included urine amino and organic acid screens, blood lactate, liver-function tests, karyotype, magnetic resonance imaging of the brain, screening for the c.35delG mutation in *GJB2* (MIM 121011), and, in the older boy, muscle and liver respiratory-chain enzyme studies and testing for several of the common mtDNA point mutations. The affected boys are currently aged 11 and 9 years. Their sister, III-1, is currently aged 13 years, is completely asymptomatic, and has normal hearing. Their parents are both healthy, and the mother has normal hearing, whereas the father has mild adult-onset hearing impairment. One of the maternal uncles, II-1, was thought to have Duchenne muscular dystrophy and died at age 2 years. He never learned to speak, and, in retrospect, it is likely that he, too, had Arts syndrome. Another maternal uncle, II-2, currently aged 27 years, had hydrocephalus of uncertain etiology, which required shunting in infancy. The third maternal uncle, II-3, died of sudden infant death syndrome at age 6 mo.

Linkage Analysis

The genetic defect in both families was linked to the X chromosome. In family N032, the 21-Mb linkage interval was previously described by Kremer et al.[30] and is flanked by the polymorphic markers *DXS1231* and *DXS1001,* with a maximum LOD score of 6.97 (fig. 1*C*). The interval contains 227 annotated genes (NCBI Map Viewer build 36.2). Mutations in known X-linked mental retardation genes *ACSL4* (MIM 300157), *AGTR2* (MIM 300034), *PAK3* (MIM 300142), and *UBE2A* (MIM 312180) were excluded by direct DNA sequencing.[29] Copy-number variations >200 kb were excluded as well by use of array comparative genomic hybridization on a full-coverage X-chromosome BAC array.[31]

For family F, an exclusion-mapping approach was taken, because a recessive X-linked defect was suspected and the family was too small to reach a significant LOD score. The uncle with hydrocephalus, II-2, was presumed to have an unrelated disorder (i.e., was considered unaffected for the purposes of this study), and the mother, II-4, and maternal grandmother, I-2, were presumed to be carriers for the disorder. Therefore, alleles not inherited from the maternal grandmother were excluded, as were alleles shared with the unaffected uncle II-2. In this way, three candidate regions were identified in this family, one of ~13 cM at Xq23 between markers *DXS1106* and *DXS8064,* which overlaps with the linkage interval of family N032 (fig. 1*B*), one ~3-cM region at Xq27 between *DXS1227* and *DXS8043* and one ~8-cM region at Xq27 between *DXS8043* and *DXS8091*. The transient receptor potential channel 5 gene (*TRPC5*), which is located within the Xq23 candidate region identified in family F, was chosen as an initial candidate gene. TRPC5 is expressed exclusively in the adult and developing CNS, and it has proposed that it forms receptor-mediated nonselective cation channels in CNS cells.[22,32–34] It is thus a candidate for mental retardation and other developmental disorders, such as Arts syndrome.[22] One change, c.919-42A→G, was identified in the affected boys in family F and in their normal father and maternal grandfather. It is therefore likely to be a common polymorphism.

Expression Profiling in Family N032

Fibroblast cell lines from two affected members of family N032, IV-2 and V-5 (for patient designation, see the work of Arts et al.[14]), were analyzed by expression profiling with the use of the GeneChip Human Genome U133 Plus 2.0 Array. The combined expression profile of the two affected family members was compared with the combined expression profile of two pools of four separate cell lines from healthy control individuals (see the tab-delimited ASCII file [online only], which can be imported into a spreadsheet). The three genes that were most reduced in expression in the linkage interval were *CUL4B, C1GALT1C1* (MIM 300611), and *PRPS1* (table 3); they were reduced in expression 1.9-fold, 1.4-fold, and 1.4-fold, respectively.

Table 3. Top 10 Probe Sets with the Most Reduced Expression in the Linkage Interval on the X Chromosome in Family N032

Probe Set	Gene	Accession Number		Expression Level	$\log_2$ Ratio	Fold Reduction
		GenBank	MIM			
210257_x_at	*CUL4B*	AF212995	300304	321	−.91	1.9
215997_s_at	*CUL4B*	AV694732	300304	277	−.81	1.8
219283_at	*C1GALT1C1*	NM_014158	300611	905	−.50	1.4
208447_s_at	*PRPS1*	NM_002764	311850	1,925	−.46	1.4
205584_at	*CXorf45*	NM_024810	...	122	−.39	1.3
201215_at	*PLS3*	NM_005032	300131	1,753	−.37	1.3
219771_at	*TBC1D8B*	NM_017752	...	223	−.37	1.3
202371_at	*TCEAL4*	NM_024863	...	1,273	−.34	1.3
219297_at	*WDR44*	NM_019045	...	156	−.29	1.2
210904_s_at	*IL13RA1*	U81380	300119	448	−.27	1.2

P values corrected for multiple testing by use of the Benjamini-Hochberg method[35] were all >.5, which was probably the result of using only four hybridizations. *C1GALT1C1* was considered an unlikely candidate gene, because somatic loss-of-function mutations in this gene cause Tn syndrome, a rare autoimmune disease in which subpopulations of blood cells of all lineages carry an incompletely glycosylated membrane glycoprotein.[36] The reduction in expression of *CUL4B* and *PRPS1* was validated by qPCR, in which the average expression of the gene of interest in the cell lines from the two affected individuals was compared with the average expression in eight separate cell lines from different control individuals. In family members IV-2 and V-5, *PRPS1* was reduced in expression 1.3-fold ($P = .68$) and 2.4-fold ($P = .22$), respectively. Although these values are only marginally lower than those of controls, they were reproducible by qPCR, and they do confirm the results of the expression array. The expression of *CUL4B* in fibroblast cell lines could not be assessed by qPCR, most likely because of its low expression level in these cells.

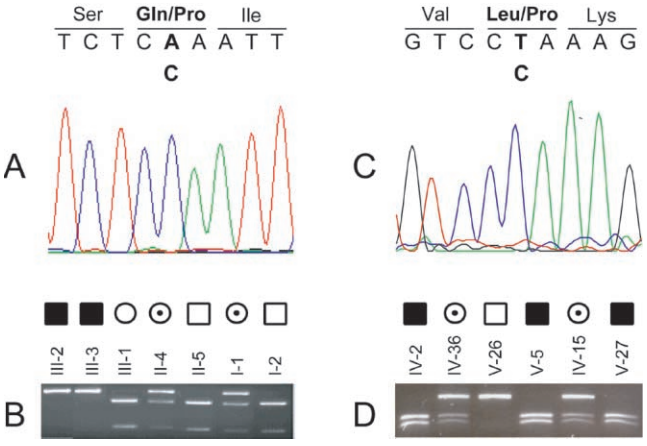

Figure 2. Chromatograms showing the nucleotide changes in *PRPS1*. *A,* c.398A→C transversion in exon 3 in individual III-2 of family F. *B,* Segregation of the mutant allele within family F (see also fig. 1*A*), as shown by *Apo*I restriction analysis. *C,* c.455T→C transition in exon 4 in individual IV-2 of family N032. *D,* Segregation of the mutant allele within family N032 (family members are numbered as in the work of Arts et al.[14]), as shown by *Bsm*FI restriction analysis.

CUL4B *and* PRPS1 *Mutation Analysis*

Recently, Tarpey et al.[37] reported that mutations in *CUL4B* cause an X-linked mental retardation syndrome associated with aggressive outbursts, seizures, relative macrocephaly, central obesity, hypogonadism, pes cavus, and tremor. Although this syndrome appears to be clearly distinct from Arts syndrome and although we could not confirm the reduction in expression by qPCR, we nevertheless analyzed all exons, intron-exon boundaries, and branch sites of the protein-coding sequence of *CUL4B* in the two affected members of family N032, IV-2 and V-5. No changes were identified (results not shown).

PRPS1 encodes PRS-I, an enzyme that catalyzes the first step in the purine metabolic pathway converting ribose-5-phosphate to PRPP. Direct DNA sequencing of the seven exons, intron-exon boundaries, and branch sites in the two affected family members IV-2 and V-5 revealed one change, c.455T→C (fig. 2*C*), that results in the substitution of a proline for a leucine at position 152 (p.L152P). This change introduces a *Bsm*FI restriction site. Restriction analysis by *Bsm*FI digestion showed that this change segregated with the disease in the family (fig. 2*D*) and was absent in 301 X chromosomes from healthy Dutch individuals (data not shown). Subsequent mutation analysis of *PRPS1* in the two affected boys from family F revealed a second mutation, c.398A→C (fig. 2*A*), which results in the substitution of proline for a glutamine at position 133 (p.Q133P). This change removes an *Apo*I restriction site. *Apo*I restriction analysis revealed that this change segregated with the disease in the family (fig. 2*B*) and was absent in 308 X chromosomes from healthy Australian individuals (data not shown).

Molecular Modeling

PRS-I amino acid residues Q133 and L152 are completely conserved among species, from human to zebrafish (UCSC

Genome Browser).[38] According to the Sorting Intolerant From Tolerant (SIFT) program,[39] which can be used to predict whether amino acid residues at a specific position in a protein can be altered, neither mutation would be tolerated at their positions. Models of PRS-I with p.L152P or p.Q133P were built on the recent crystal structure of human PRS-I[23] (fig. 3). PRS-I is believed to be physiologically functional as a hexamer, which consists of three homodimers arranged in a propeller-like shape (fig. 3*A* and 3*B*). Q133 is positioned at the interface of the two monomers of a homodimer and forms a hydrogen bond to D98 from the other unit in the homodimer (fig. 3*A*). Thus, the p.Q133P mutation disrupts two of the intermolecular hydrogen bonds between the two monomers (fig. 3*C* and 3*E*). As a consequence, both the homodimer and the allosteric site would be destabilized. In addition, Q133 and especially its hydrogen-bonding partner D98 are in close proximity to the ATP-binding pocket. The neighboring amino acid residues R96, Q97, K99, and D101 all interact with the incoming ATP molecule; therefore, the loss of the hydrogen-bonding partner of D98 could also destabilize the ATP-binding pocket and thus impair PRS-I activity. L152 is positioned in the middle of one of the α-helixes (fig. 3*D*). Replacement of this leucine with a proline will break this α-helix configuration (fig. 3*F*) and, consequently, will destabilize the protein structure.

PRPP Synthetase Activity in Erythrocytes, Fibroblasts, and EBV-LCLs

PRPP synthetase activity was measured in erythrocytes from the two patients, III-2 and III-3; the mother, II-4; the sister who is not a carrier, III-1; and the father, II-5, from family F (table 4). There was no activity in erythrocytes from the affected boys. The activity in their mother, 18 nmol/mg/h, was outside the normal range (24–48 nmol/mg/h). In both family members without the mutation, the PRPP synthetase activity was normal. A repeat analysis of the test gave comparable results.

PRPP synthetase activity was measured in cultured skin fibroblasts from three affected members of family N032, IV-2, V-5, and V-27, and from one affected member of family F, III-2. The PRPP synthetase activity in the patient fibroblasts was compared with that in fibroblasts from eight unrelated healthy control individuals. The activity in the three patients from family N032 was, on average, 13-fold reduced ($P < .05$, calculated by Student's t test) compared with the average PRPP synthetase activity in fibroblasts from controls (table 5). The activity in fibroblasts from the patient in family F was equally reduced.

PRPP synthetase activity was also determined in EBV-LCLs from two carrier females, IV-28 and IV-36, and an unaffected male, V-10, from family N032. The enzyme activities in EBV-LCLs from two unrelated healthy control individuals were analyzed as additional controls. In carrier females, the PRPP synthetase activity was 486 and 392 nmol/mg/h, which was lower than the activity in the unaffected male family member, 664 nmol/mg/h, and that in the two controls, 519 and 636 nmol/mg/h. This reduction in PRPP synthetase activity was not statistically significant.

Metabolite Analysis

Serum uric acid levels lower than average were found in patients and carrier females in family F, with values at the lower limit of the reference range for age and sex (table 4). Purine urinary profiles of the Australian boys were unusual, in that hypoxanthine was below the level of detection, whereas xanthine was relatively normal. Urine uric acid excretion was within the normal range for age. It should be noted that excreted uric acid, unlike hypoxanthine and xanthine, arises from dietary sources as well as from endogenous metabolism. All other purine and pyrimidine metabolites appeared to be within the normal ranges. An unidentified metabolite with a spectral maximum at ~265 nm was noticed in urine from the affected boys, but its origin was undetermined.

Discussion

In two families with Arts syndrome, we have identified two mutations (p.Q133P and p.L152P) in *PRPS1*. Both mutations result in a loss of PRS-I activity, as shown both *in silico* by molecular modeling and in vitro by PRPP synthetase activity assays in erythrocytes, fibroblasts, and EBV-LCLs. It is also reflected by the undetectable urine hypoxanthine and reduced plasma uric acid levels in the two patients from family F. Interestingly, the p.L152P mutation also seems to cause a small reduction of ~1.8-fold in *PRPS1* transcript levels, which would be predicted to cause a reduction in the protein levels in addition to the reduction in the protein activity. The p.Q133P mutation did not cause reduced expression levels (data not shown). Notably, *PRPS2* expression levels were not elevated in fibroblasts from patients of family N032 (data not shown).

PRPS1 was selected as a candidate gene by a strategy comprising expression profiling. The principle behind this strategy was to identify small deletions or mutations that lead to nonsense-mediated RNA decay. It is surprising, therefore, that a missense mutation was identified in *PRPS1*. It is possible that this missense mutation is directly responsible for the slightly reduced *PRPS1* expression—for example, by introducing a less favorable codon for the translation machinery, the disruption of secondary structures in the mRNA, or feedback/feedforward mechanisms. However, we cannot exclude that the mutation is irrelevant to the reduced *PRPS1* expression levels and that our selection of the gene was a fortuitous event.

PRPP synthetase enzyme activity is totally absent in erythrocytes from patients of family F, whereas residual activity was observed in fibroblasts from one of these patients. This suggests that the PRS-I activity in erythrocytes is more severely impaired than that in fibroblasts. The

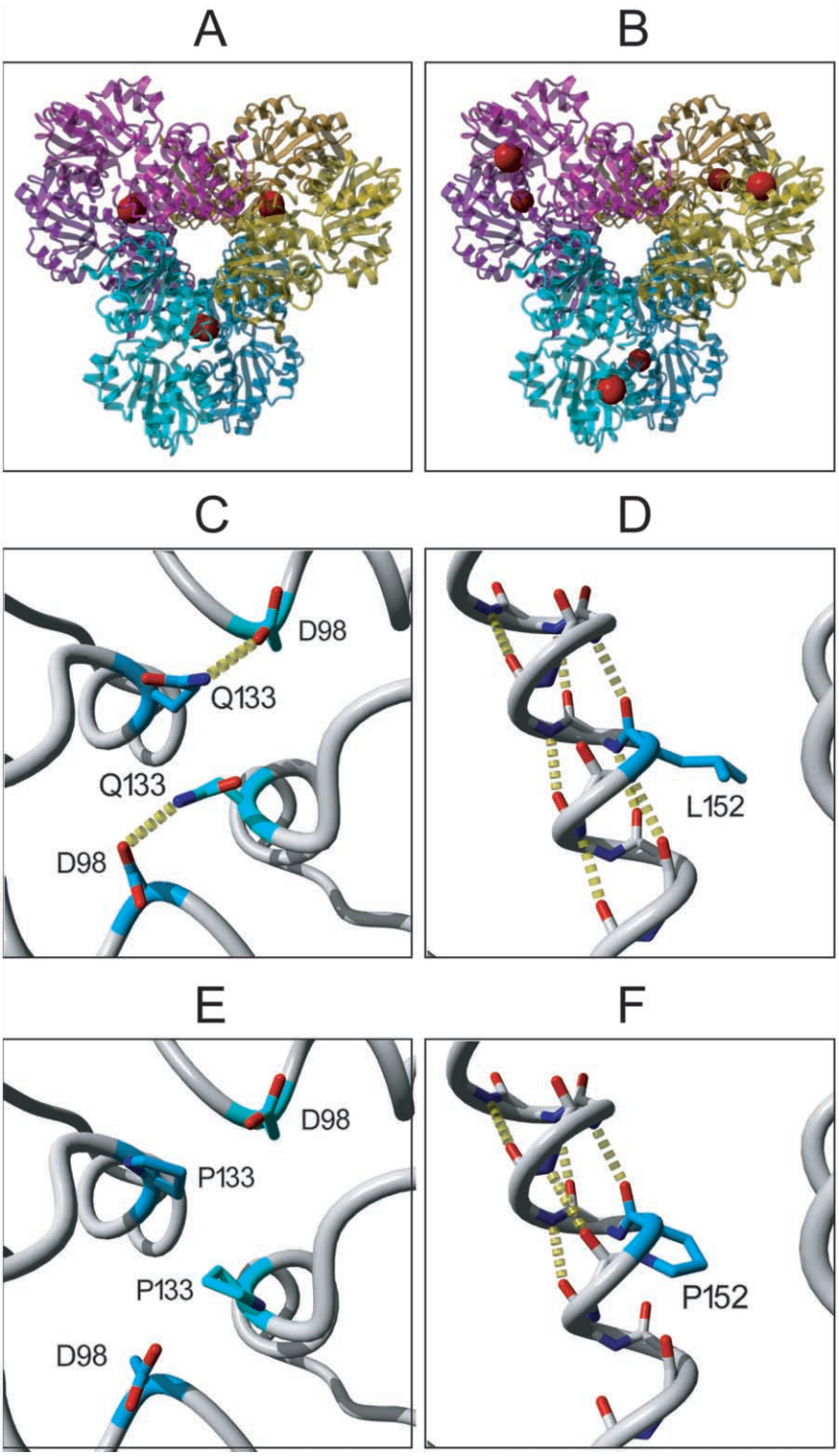

Figure 3. Three-dimensional model of PRS-I as a hexamer (*A* and *B*) and close-ups of the two regions of PRS-I that contain the mutations p.Q133P (*C* and *E*) and p.L152P (*D* and *F*). The red spheres indicate the positions of the mutated amino acid residues in the PRS-I hexamer. The yellow dotted lines represent the hydrogen bonds.

Table 4. PRPP Synthetase Activity in Erythrocytes and Purine Metabolite Levels in Serum and Urine from Members of Family F and Two Control Individuals

Individual	Sex	Mutation Carrier	Activity[a] (nmol/mg/h)	Serum Uric Acid[b] (mM)	Urine[c] (mmol/mol creatine)		
					Hypoxanthine	Xanthine	Uric Acid
Family F:							
III-1	F	No	28	.24	10 [2–55]	8 [5–80]	260 [200–600]
III-2	M	Yes	0	.13	<1 [2–55]	8 [5–80]	490 [200–600]
III-3	M	Yes	0	.16	<1 [2–55]	10 [5–80]	540 [300–1,000]
II-4	F	Yes	18	.16	6 [5–30]	4 [5–30]	320 [200–500]
II-5	M	No	40	.37	11 [5–30]	6 [5–30]	250 [200–500]
Control:							
1	M	No	52	…	…	…	…
2	M	No	55	…	…	…	…

[a] The normal range for PRPP synthetase activity in erythrocytes is 24–48 nmol/mg/h.
[b] The normal range for serum uric acid levels is 0.12–0.35 mM.
[c] Age- and sex-dependent normal ranges for the urine metabolites are given in brackets.

erythrocyte presents unique challenges to the stability of its constituent proteins. In addition to being unable to synthesize new proteins, the erythrocyte is subject to powerful oxidative free radicals. This environment has been demonstrated to result in loss of function of other enzymes containing destabilizing mutations, particularly in thalassemia.[40] The lack of PRS-I activity in erythrocytes but not in fibroblasts likely reflects a reduced stability of mutant PRS-I protein compared with that of normal PRS-I. Indeed, a destabilization of PRS-I protein complexes was predicted by the structural models.

Until now, mutations identified in *PRPS1* were all missense mutations that cause a superactivity of the protein. Patients with PRPP synthetase superactivity all have hyperuricemia and/or gout.[1,41] In contrast to the two novel loss-of-function missense mutations described here, molecular modeling showed that the gain-of-function missense mutations are present in the dimer-trimer interface (data not shown), which results in impairment of the allosteric inhibition of PRS-I by purine nucleotides and free phosphate.[7–10,42] PRPS-related gout is characterized by purine nucleotide and uric acid overproduction,[5–7] gout,[6,8] and sometimes severe neurodevelopmental impairment.[8–11] Progressive axonal neuropathy with demyelination has been described in one family.[43] Neurological abnormalities, such as mental retardation, ataxia, hearing impairment, and areflexia, that overlap between patients with Arts syndrome and those with PRPS-related gout (table 2) indicate that these symptoms are a direct effect of changes in PRS-I activity.

Table 5. PRPP Synthetase Activity in Fibroblasts from Patients and Healthy Unrelated Control Individuals

Individual	Sex	Mutation Carrier	Activity (nmol/mg/h)
Family N032:			
IV-2	M	Yes	1.3
V-5	M	Yes	1.1
V-27	M	Yes	0
Family F:			
III-2	M	Yes	.4
Control:			
1	F	No	20.9
2	F	No	6.3
3	F	No	9.9
4	M	No	14.6
5	M	No	6.3
6	M	No	16.8
7	M	No	.6
8	M	No	.3

PRS-I catalyzes the first step in the purine metabolic pathway converting ribose-5-phosphate to PRPP. PRPP is synthesized solely via PRS-I and/or PRS-II and is essential for the de novo synthesis of purines and pyrimidines, as well as for salvage of purines. The mutations in *PRPS1* that we have described here should, consequently, result in relatively low purine nucleotides in general, which is reflected in the reduced serum uric acid levels, although these levels are subject to diet, and in the low excretion of urinary hypoxanthine in the two patients of family F. Although PRPP is also a substrate used in pyrimidine metabolism, pyrimidine nucleotides would not be expected to be affected as severely as purine nucleotides, because PRPP is not essential for pyrimidine salvage, as it is for purine salvage. In addition, dietary pyrimidine nucleosides are able to cross the gut. However, we would predict that the overall intracellular purine and pyrimidine nucleotide levels in these patients would be lower than normal, which would mean that Arts syndrome is the first identified inborn error that affects both purine and pyrimidine biosynthesis. Indeed, patients with Arts syndrome do show symptoms that can be attributed to both lower purine and lower pyrimidine nucleotide levels. Developmental delay, for instance, is thought to be caused by a shortage of guanosine triphosphate (GTP) in Lesch-Nyhan syndrome (MIM 300322).[12] Immunodeficiency occurs in two purine disorders—namely, adenosine deaminase deficiency (MIM 102700) and PNP deficiency.[12] ATP is critical for the high-energy requirements of bone mar-

row, and GTP for lymphocyte maturation. Other tissues with high-energy requirements, such as the brain and retina, would then also be predicted to be affected. Demyelination may be a result of a reduction in pyrimidine nucleotides, which are essential for membrane and myelin synthesis and deposition through their lipid esters (e.g., cytidine-5′-phospho [CDP]–choline and CDP-ethanolamine).[44] Taken together, depletion of both purines and pyrimidines would give rise to the complex and severe Arts syndrome phenotype.

Although PRPP synthetases are crucial for de novo purine synthesis, specifically ATP can be generated by an alternative pathway utilizing *S*-adenosylmethionine (SAM) as a substrate, as has been demonstrated in human erythrocytes.[45–48] Methyltransferases convert SAM into *S*-adenosylhomocysteine that, in turn, is hydrolyzed by *S*-adenosylhomocysteine hydrolase, to yield adenosine and L-homocysteine. This introduces an alternative source of adenosine that is salvaged through adenosine kinase into adenosine nucleotides.[49] Purine nucleotide recycling can then convert the SAM-derived adenosine nucleotides into guanosine nucleotides. Importantly, SAM appears to be unique among purines in that it can pass across the gut, where dietary purines are normally oxidized to uric acid.[50] Furthermore, SAM also has been shown to pass the blood-brain barrier. Supplementary SAM has been used safely in the treatment of depression, neurologic disorders, liver disease, and osteoarthritis.[51] Recently, a patient with Lesch-Nyhan syndrome was shown to benefit clearly from SAM administration, without untoward side effects.[52] This suggests that low GTP levels can also be elevated by SAM. One of us (J.A.D.) hypothesizes that supplementary SAM in the diet of our PRS-I–deficient patients could perhaps alleviate the clinical symptoms caused by a shortage of specifically adenosine-derived nucleotides. In addition, SAM is also a source of methionine, which could overcome a possible deficiency of methylation processes caused by low ATP levels and thus low endogenous SAM levels, because SAM synthesis is ATP dependent. By relieving the stress on purine nucleotides, it is possible theoretically to reduce the effects of pyrimidine nucleotide depletion. Dietary pyrimidines, unlike purines, are absorbed into the body and then salvaged as nucleosides, principally from uridine.[53] We have begun dietary supplementation with SAM in the Australian patients and may consider uridine supplementation if indicated, although we predict that dietary uridine may be sufficient.

In summary, PRS-I loss-of-function mutations cause Arts syndrome. The clinical presentation is reminiscent of symptoms seen in other purine and pyrimidine disorders. We propose that these symptoms are the result of nucleotide depletion in key energy-requiring tissues. A deficiency in purine nucleotides could theoretically be compensated partially by supplementary SAM, and a trial of SAM is currently under way in the two affected Australian males.

Acknowledgments

We thank Dr. Willem F. Arts for ascertaining the Dutch family. In addition, we are grateful to Dr. Kevin Carpenter (New South Wales Biochemical Genetics Service, Sydney), for his assistance in the preparation and dispatch of samples for analyses, and Saskia van der Velde (Department of Human Genetics, Radboud University Nijmegen Medical Centre, Nijmegen), for technical assistance with cell culturing.

Web Resources

Accession numbers and URLs for data presented herein are as follows:

GenBank, http://www.ncbi.nlm.nih.gov/Genbank/ (for accession numbers NM_003588.3, NM_002764.2, and NM_012471.2 and those in tables 1 and 3)
NCBI Map Viewer, http://www.ncbi.nlm.nih.gov/mapview/ (for build 36.2)
Online Mendelian Inheritance in Man (OMIM), http://www.ncbi.nlm.nih.gov/Omim/ (for *PRPS1, PRPS2,* PRPS-related gout, orotic aciduria, Arts syndrome, HPRT1 deficiency, PNP deficiency, *GUSB, CUL4B, TRPC5, GJB2, ACSL4, AGTR2, PAK3, UBE2A, C1GALT1C1, PLS3, IL13RA1,* Lesch-Nyhan syndrome, and adenosine deaminase deficiency)
Primer3, http://frodo.wi.mit.edu/cgi-bin/primer3/primer3_www.cgi
RCSB Protein Data Bank, http://www.pdb.org/
SIFT, http://blocks.fhcrc.org/sift/SIFT.html
UCSC Genome Browser, http://www.genome.ucsc.edu/
YASARA, http://www.yasara.org/

References

1. Becker MA (2001) Phosphoribosylpyrophosphate synthetase and the regulation of phosphoribosylpyrophosphate production in human cells. Prog Nucleic Acid Res Mol Biol 69:115–148
2. Becker MA, Heidler SA, Bell GI, Seino S, Le Beau MM, Westbrook CA, Neuman W, Shapiro LJ, Mohandas TK, Roessler BJ (1990) Cloning of cDNAs for human phosphoribosylpyrophosphate synthetases 1 and 2 and X chromosome localization of PRPS1 and PRPS2 genes. Genomics 8:555–561
3. Taira M, Iizasa T, Yamada K, Shimada H, Tatibana M (1989) Tissue-differential expression of two distinct genes for phosphoribosyl pyrophosphate synthetase and existence of the testis-specific transcript. Biochim Biophys Acta 1007:203–208
4. Becker MA, Taylor W, Smith PR, Ahmed M (1996) Overexpression of the normal phosphoribosylpyrophosphate synthetase 1 isoform underlies catalytic superactivity of human phosphoribosylpyrophosphate synthetase. J Biol Chem 271: 19894–19899
5. Becker MA, Losman MJ, Kim M (1987) Mechanisms of accelerated purine nucleotide synthesis in human fibroblasts with superactive phosphoribosylpyrophosphate synthetases. J Biol Chem 262:5596–5602
6. Sperling O, Boer P, Persky-Brosh S, Kanarek E, De Vries A (1972) Altered kinetic property of erythrocyte phosphoribosylpyrophosphate synthetase in excessive purine production. Rev Eur Etud Clin Biol 17:703–706
7. Zoref E, De Vries A, Sperling O (1975) Mutant feedback-resistant phosphoribosylpyrophosphate synthetase associated with purine overproduction and gout: phosphoribosylpyro-

phosphate and purine metabolism in cultured fibroblasts. J Clin Invest 56:1093–1099
8. Becker MA, Puig JG, Mateos FA, Jimenez ML, Kim M, Simmonds HA (1988) Inherited superactivity of phosphoribosylpyrophosphate synthetase: association of uric acid overproduction and sensorineural deafness. Am J Med 85:383–390
9. Becker MA, Raivio KO, Bakay B, Adams WB, Nyhan WL (1980) Variant human phosphoribosylpyrophosphate synthetase altered in regulatory and catalytic functions. J Clin Invest 65: 109–120
10. Becker MA, Smith PR, Taylor W, Mustafi R, Switzer RL (1995) The genetic and functional basis of purine nucleotide feedback-resistant phosphoribosylpyrophosphate synthetase superactivity. J Clin Invest 96:2133–2141
11. Simmonds HA, Webster DR, Lingam S, Wilson J (1985) An inborn error of purine metabolism, deafness and neurodevelopmental abnormality. Neuropediatrics 16:106–108
12. Nyhan WL (2005) Disorders of purine and pyrimidine metabolism. Mol Genet Metab 86:25–33
13. Page T, Yu J, Fontanesi WL, Nyhan WL (1997) Developmental disorder associated with increased cellular nucleotidases activity. Proc Natl Acad Sci USA 94:11601–11606
14. Arts WF, Loonen MC, Sengers RC, Slooff JL (1993) X-linked ataxia, weakness, deafness, and loss of vision in early childhood with a fatal course. Ann Neurol 33:535–539
15. Miller SA, Dykes DD, Polesky HF (1988) A simple salting out procedure for extracting DNA from human nucleated cells. Nucleic Acids Res 16:1215
16. Weaving LS, Williamson SL, Bennetts B, Davis M, Ellaway CJ, Leonard H, Thong MK, Delatycki M, Thompson EM, Laing N, et al (2003) Effects of *MECP2* mutation type, location and X-inactivation in modulating Rett syndrome phenotype. Am J Med Genet A 118:103–114
17. Wall FE, Henkel RD, Stern MP, Jenson HB, Moyer MP (1995) An efficient method for routine Epstein-Barr virus immortalization of human B lymphocytes. In Vitro Cell Dev Biol Anim 31:156–159
18. Rozen S, Skaletsky H (2000) Primer3 on the WWW for general users and for biologist programmers. Methods Mol Biol 132: 365–386
19. de Brouwer AP, van Bokhoven H, Kremer H (2006) Comparison of 12 reference genes for normalization of gene expression levels in Epstein-Barr virus-transformed lymphoblastoid cell lines and fibroblasts. Mol Diagn Ther 10:197–204
20. Livak KJ, Schmittgen TD (2001) Analysis of relative gene expression data using real-time quantitative PCR and the $2^{-\Delta\Delta C_T}$ method. Methods 25:402–408
21. Pfaffl MW (2001) A new mathematical model for relative quantification in real-time RT-PCR. Nucleic Acids Res 29:e45
22. Sossey-Alaoui K, Lyon JA, Jones L, Abidi FE, Hartung AJ, Hane B, Schwartz CE, Stevenson RE, Srivastava AK (1999) Molecular cloning and characterization of TRPC5 (HTRP5), the human homologue of a mouse brain receptor-activated capacitative Ca^{2+} entry channel. Genomics 60:330–340
23. Li S, Lu Y, Peng B, Ding J (2007) Crystal structure of human phosphoribosylpyrophosphate synthetase 1 reveals a novel allosteric site. Biochem J 401:39–47
24. Krieger E, Darden T, Nabuurs SB, Finkelstein A, Vriend G (2004) Making optimal use of empirical energy functions: force-field parameterization in crystal space. Proteins 57:678–683
25. Montero C, Duley JA, Fairbanks LD, McBride MB, Micheli V, Cant AJ, Morgan G (1995) Demonstration of induction of erythrocyte inosine monophosphate dehydrogenase activity in Ribavirin-treated patients using a high performance liquid chromatography linked method. Clin Chim Acta 238:169–178
26. Smith PK, Krohn RI, Hermanson GT, Mallia AK, Gartner FH, Provenzano MD, Fujimoto EK, Goeke NM, Olson BJ, Klenk DC (1985) Measurement of protein using bicinchoninic acid. Anal Biochem 150:76–85
27. Torres RJ, Mateos FA, Puig JG, Becker MA (1996) Determination of phosphoribosylpyrophosphate synthetase activity in human cells by a non-isotopic, one step method. Clin Chim Acta 245:105–112
28. Simmonds HA, Duley JA, Davies PM (1990) Analysis of purines and pyrimidines in blood, urine and other physiological fluids. In: Hommes FA (ed) Techniques in diagnostic human biochem genetics. Wiley-Liss, New York, pp 397–424
29. de Brouwer AP, Yntema HG, Kleefstra T, Lugtenberg D, Oudakker AR, de Vries BB, van Bokhoven H, Van Esch H, Frints SG, Froyen G, et al (2007) Mutation frequencies of X-linked mental retardation genes in families from the EuroMRX consortium. Hum Mutat 28:207–208
30. Kremer H, Hamel BC, van den Helm B, Arts WF, de Wijs IJ, Sistermans EA, Ropers HH, Mariman EC (1996) Localization of the gene (or genes) for a syndrome with X-linked mental retardation, ataxia, weakness, hearing impairment, loss of vision and a fatal course in early childhood. Hum Genet 98: 513–517
31. Lugtenberg D, de Brouwer AP, Kleefstra T, Oudakker AR, Frints SG, Schrander-Stumpel CT, Fryns JP, Jensen LR, Chelly J, Moraine C, et al (2006) Chromosomal copy number changes in patients with non-syndromic X linked mental retardation detected by array CGH. J Med Genet 43:362–370
32. Benjamini Y, Hochberg Y (1995) Controlling the false discovery rate: a practical and powerful approach to multiple testing. J R Stat Soc B 57:289–300
33. Ju T, Cummings RD (2005) Protein glycosylation: chaperone mutation in Tn syndrome. Nature 437:1252
34. Plant TD, Schaefer M (2003) TRPC4 and TRPC5: receptor-operated Ca^{2+}-permeable nonselective cation channels. Cell Calcium 33:441–450
35. Riccio A, Medhurst AD, Mattei C, Kelsell RE, Calver AR, Randall AD, Benham CD, Pangalos MN (2002) mRNA distribution analysis of human TRPC family in CNS and peripheral tissues. Brain Res Mol Brain Res 109:95–104
36. Schaefer M, Plant TD, Obukhov AG, Hofmann T, Gudermann T, Schultz G (2000) Receptor-mediated regulation of the nonselective cation channels TRPC4 and TRPC5. J Biol Chem 275: 17517–17526
37. Tarpey PS, Raymond FL, O'Meara S, Edkins S, Teague J, Butler A, Dicks E, Stevens C, Tofts C, Avis T, et al (2007) Mutations in *CUL4B,* which encodes a ubiquitin E3 ligase subunit, cause an X-linked mental retardation syndrome associated with aggressive outbursts, seizures, relative macrocephaly, central obesity, hypogonadism, pes cavus, and tremor. Am J Hum Genet 80:345–352
38. Siepel A, Bejerano G, Pedersen JS, Hinrichs AS, Hou M, Rosenbloom K, Clawson H, Spieth J, Hillier LW, Richards S, et al (2005) Evolutionarily conserved elements in vertebrate, insect, worm, and yeast genomes. Genome Res 15:1034–1050
39. Ng PC, Henikoff S (2002) Accounting for human polymor-

phisms predicted to affect protein function. Genome Res 12: 436–446
40. Rees DC, Duley J, Simmonds HA, Wonke B, Thein SL, Clegg JB, Weatherall DJ (1996) Interaction of hemoglobin E and pyrimidine 5′ nucleotidase deficiency. Blood 88:2761–2767
41. Garcia-Pavia P, Torres RJ, Rivero M, Ahmed M, Garcia-Puig J, Becker MA (2003) Phosphoribosyl pyrophosphate synthetase overactivity as a cause of uric acid overproduction in a young woman. Arthritis Rheum 48:2036–2041
42. Becker MA, Losman MJ, Wilson J, Simmonds HA (1986) Superactivity of human phosphoribosyl pyrophosphate synthetase due to altered regulation by nucleotide inhibitors and inorganic phosphate. Biochim Biophys Acta 882:168–176
43. Christen HJ, Hanefeld F, Duley JA, Simmonds HA (1992) Distinct neurological syndrome in two brothers with hyperuricaemia. Lancet 340:1167–1168
44. Ross BM, Moszczynska A, Blusztajn JK, Sherwin A, Lozano A, Kish SJ (1997) Phospholipid biosynthetic enzymes in human brain. Lipids 32:351–358
45. Montero C, Smolenski RT, Duley JA, Simmonds HA (1990) S-adenosylmethionine increases erythrocyte ATP in vitro by a route independent of adenosine kinase. Biochem Pharmacol 40:2617–2623
46. Simmonds HA, Fairbanks LD, Duley JA, Morris GS (1989) ATP formation from deoxyadenosine in human erythrocytes: evidence for a hitherto unidentified route involving adenine and S-adenosylhomocysteine hydrolase. Biosci Rep 9:75–85
47. Smolenski RT, Montero C, Duley JA, Simmonds HA (1991) Effects of adenosine analogues on ATP concentrations in human erythrocytes: further evidence for a route independent of adenosine kinase. Biochem Pharmacol 42:1767–1773
48. Smolenski RT, Fabianowska-Majewska K, Montero C, Duley JA, Fairbanks LD, Marlewski M, Simmonds HA (1992) A novel route of ATP synthesis. Biochem Pharmacol 43:2053–2057
49. Schuster S, Kenanov D (2005) Adenine and adenosine salvage pathways in erythrocytes and the role of *S*-adenosylhomocysteine hydrolase: a theoretical study using elementary flux modes. FEBS J 272:5278–5290
50. Stow RA, Bronk JR (1993) Purine nucleoside transport and metabolism in isolated rat jejunum. J Physiol 468:311–324
51. Bottiglieri T (2002) *S*-adenosyl-L-methionine (SAMe): from the bench to the bedside—molecular basis of a pleiotrophic molecule. Am J Clin Nutr 76:1151S–1157S
52. Glick N (2006) Dramatic reduction in self-injury in Lesch-Nyhan disease following *S*-adenosylmethionine administration. J Inherit Metab Dis 29:687
53. Becroft DM, Phillips LI, Simmonds A (1969) Hereditary orotic aciduria: long-term therapy with uridine and a trial of uracil. J Pediatr 75:885–891